Applied Catalysis B: Environmental 96 (2010) 548–556

Contents lists available at ScienceDirect

Applied Catalysis B: Environmental

journal homepage: www.elsevier.com/locate/apcatb

Removal of Reactive Black 5 azo dye from aqueous solutions by catalytic oxidation using CuO/Al_2O_3 and NiO/Al_2O_3

Corina Bradu [a,*], Ligia Frunza [b], Nicoleta Mihalche [a], Sorin-Marius Avramescu [a], Marian Neaţă [a], Ion Udrea [a]

[a] Organic Chemistry Department, University of Bucharest, Bd. Regina Elisabeta 4-12, Sect. 3, Bucharest 030018, Romania
[b] National Institute of Materials Physics, Str. Atomistilor 105 bis, Magurele 077125, Romania

ARTICLE INFO

Article history:
Received 13 November 2009
Received in revised form 24 February 2010
Accepted 1 March 2010
Available online 17 March 2010

Keywords:
Azo dye removal
Catalytic oxidation
Advanced oxidation processes
Reactive Black 5

ABSTRACT

CuO/Al_2O_3 and NiO/Al_2O_3 catalysts prepared by incipient wetness impregnation were used for the oxidation of Reactive Black 5 (RB5) in aqueous solution. Removal of the dye was assessed by High Performance Liquid Chromatography (HPLC) and Total Organic Carbon (TOC) measurements and the generation of the hydroxyl radicals in the process was evaluated by chemiluminescence measurements. To put in evidence the interaction RB5 – catalyst and the surface species formed onto catalysts during the oxidation, Diffuse Reflectance Infrared Fourier Transform (DRIFT) analysis was performed. A different behavior of the two catalytic systems was revealed by the comparative analysis of the data obtained from the adsorption and oxidation tests. Only CuO/Al_2O_3 was effective in the RB5 degradation, NiO/Al_2O_3 acted as a simple adsorbent. In the presence of CuO/Al_2O_3, at H_2O_2 concentration of 40 mM the azo dye was totally eliminated from both solution and catalyst surface after 4 h, with a mineralization degree higher than 90%. However, a strong inhibition of the catalytic oxidation of RB5 was observed in the presence of phosphate ions. In the conditions of hydrogen peroxide excess, the rate equation in the case of copper catalyst was simply expressed by a pseudo-first order equation and the model was found to fit well the data. The amount of copper leached from catalyst during the oxidation process was only 1.0–1.6% per cycle leading to the conclusion that the decrease of the dye mineralization with the number of cycles has to be explained mostly by the surface covering with the reaction products, at least to a certain extent.

1. Introduction

Extensive use of reactive dyes has a strong impact especially on aquatic ecosystems, leading to their imbalance. These dyes are designed to resist to physical, chemical and microbial attack and consequently they are hard to be removed from wastewater [1]. In addition, they are susceptible to generate in the environment aromatic amines with potential carcinogenic character [2,3]. The complete mineralization of organic pollutants is the most suitable way to diminish the environmental impact. For this reason a priority over the last few years becomes the development and the evaluation of some advanced oxidation processes (AOPs), characterized by the generation of hydroxyl radicals, which are highly reactive and non-selective oxidants [4,5]. Among these processes, catalytic oxidation using powerful oxidants such as ozone or hydrogen peroxide is known to be effective in removing a number of persistent organic pollutants refractory to conventional oxidation [6]. The catalytic process can be carried out in homogeneous systems (soluble salts of transitional metals) or heterogeneous systems (solid catalyst such as supported transitional metals or metal oxides) [7–16]. The soluble salts of some transitional metals are generally efficient catalysts in this respect, but their recovering from the treated effluents is rather difficult and requires additional separation steps inducing an increase in the wastewater treatment cost. This disadvantage can be overcame by using heterogeneous catalysts if they are stable in the reaction medium [17].

As considering the degradation of azo dyes, AOPs using ozone or hydrogen peroxide represent a powerful mean to destroy the chromophoric system of these dyes as well and even to achieve high mineralization degree [18,19]. Homogeneous, Fenton- and photo-Fenton-systems are extensively used AOPs to degrade azo dyes from wastewater, their efficiency was proved in a series of works [20,21]. Copper, cobalt, nickel, manganese and other soluble salts were also tested for the oxidative degradation of azo dyes [22,23]: in the photo-oxidation of Acid Red D with H_2O_2 it was found [22] that copper and cobalt ions present good catalytic activity within a

* Corresponding author. Tel.: +40 21 4105440; fax: +40 21 4105440.
E-mail addresses: corina.bradu@g.unibuc.ro, corinabradu@yahoo.com (C. Bradu), lfrunza@infim.ro (L. Frunza), nic_mihalache@yahoo.com (N. Mihalche), sorin.avramescu@g.unibuc.ro (S.-M. Avramescu), neatamarian@yahoo.com (M. Neaţă), ion.udrea@g.unibuc.ro (I. Udrea).

0926-3373/$ – see front matter © 2010 Elsevier B.V. All rights reserved.
doi:10.1016/j.apcatb.2010.03.019

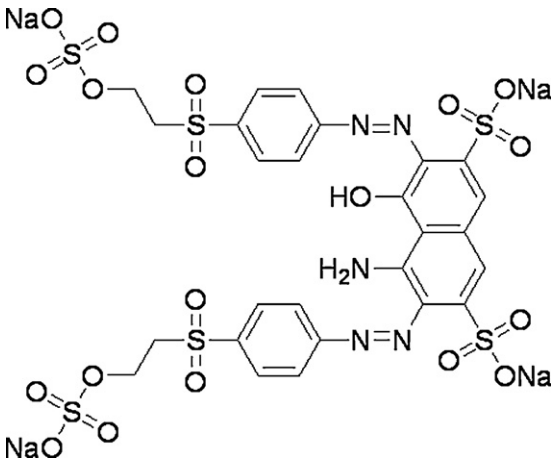

Fig. 1. Molecular structure of RB5.

wide pH range, while nickel and manganese ions have only a weak activity in alkaline media.

However, the actual trend is to develop heterogeneous systems working under mild conditions.

Metal oxides supported on alumina or silica [24–27], metal exchanged Y zeolites [28,29], metal doped carbon aerogels [30,31] or metal-polymer complexes [32], where metal is often Fe, Cu, Ni or Co, are examples of catalytic systems found to by active in the oxidative degradation of azo dye with hydrogen peroxide.

In this work, the oxidation of Reactive Black 5 (RB5) in aqueous solution with hydrogen peroxide over CuO/Al_2O_3 and NiO/Al_2O_3 catalysts is presented. We have comparatively evaluated the capacity of the two catalytic systems in RB5 removal and in the generation of hydroxyl radicals. Experiments were also carried out to investigate the effects of hydrogen peroxide dose and of the phosphate ions presence on the process evolution.

2. Experimental

2.1. Catalysts and materials

The catalysts were prepared by incipient wetness impregnation. In short, the preparation contains the following steps: impregnation of γ-Al_2O_3 with nickel or copper nitrate aqueous solutions, followed by the precursor drying at 110 °C for 4 h and calcination at 550 °C for 2 h repeated in several cycles. Details of their synthesis and characterization have been elsewhere described [33]. Some physical properties of the catalysts are presented in Table 1.

The azo dye RB5 was purchased from Sigma–Aldrich and used without further purification. Its structure is presented in Fig. 1.

2.2. Methods

2.2.1. Oxidation tests

Degradation of RB5 was investigated during a series of batch experiments. In these oxidation tests, 100 mL of RB5 solution (100 mg L^{-1}) was continuously mixed (at 150 rpm) with 0.20 g catalyst, in a closed glass vessel at temperature of 21 ± 1 °C using a thermostated shaker (*GFL 3033* type). The experiments were conducted at pH 5.5 without additional pH correction, using H_2O_2 concentration from 10 to 60 mM.

2.2.2. H_2O_2 decomposition

The decomposition of the H_2O_2 in the presence of CuO/Al_2O_3 was evaluated for a concentration solution of 40 mM. The reaction was carried out under the same experimental conditions as for RB5 oxidation tests.

2.2.3. RB5 adsorption

Adsorption tests for the RB5 onto the catalysts were also performed in conditions similar to oxidation reaction but several dye concentrations (from 10 to 500 mg L^{-1}) were used for RB5 solutions. The adsorption equilibrium was considered reached after 4 h.

2.2.4. Analytical methods

Removal of the dye was assessed by High Performance Liquid Chromatography (HPLC) method and Total Organic Carbon (TOC) measurements. For the chromatographic analysis a *Varian ProStar* apparatus equipped with an UV Diode Array detector (at λ = 599 nm) was employed. A Metacarb 67 H column (oven temperature of 40 °C) was used. The mobile phase was a solution of H_2SO_4 (0.1 M) flowing with 0.8 mL min^{-1}. TOC measurements were achieved by high temperature oxidation method using a *HiPerTOC Thermo Electron* analyzer.

During the reaction, the hydrogen peroxide concentration was determined by spectrophotometric titanium sulfate method [34]. This consists in mixing the titanium reagent ($Ti(SO_4)_2$ in H_2SO_4 solution) with the sample, which contains residual hydrogen peroxide, and allowing to react for 5 min. The absorbance of the resulted pertitanic acid was measured at λ = 405 nm with a double beam spectrophotometer *Unicam Helios α*. Our samples having higher H_2O_2 concentration were previously diluted.

The total amount of copper leached into the solution was determined using a *Thermo Elemental – Solaar M5* atomic absorption spectrometer.

Prior to analysis, all the samples collected during the runs were filtered through 0.20 μm cellulose syringe filters.

Diffuse Reflectance Infrared Fourier Transform (DRIFT) analysis was performed to put in evidence the interaction of RB5 with the catalyst and the surface species formed onto catalysts during the oxidation. The IR spectra were collected in the region 4000–500 cm^{-1} at a resolution of 2 cm^{-1} using a *Varian 3100 Excalibur* spectrometer equipped with a *Harrick Praying Mantis* diffuse reflectance accessory. These spectra were refined by subtracting the spectrum of the fresh catalyst and then analyzed with the program *Analyzer IR – KnowItAll (Bio-Rad 2005)*.

The formation of the metal-dye complex was pursued by UV–vis spectrometry using a *Unicam Helios α* spectrophotometer.

The capacity of catalysts to generate hydroxyl radicals was evaluated using the chemiluminescence system 5-amino-2,3-dihydro-1,4-phthalazinedione (luminol) – hydrogen peroxide in alkaline solution. The concentration was 10^{-4} M for luminol (200 μL) and 10^{-3} M for H_2O_2 (50 μL); the pH 8.5 was ensured by 750 μL of Tris–HCl buffer [35]. The chemiluminescence blue signal (λ = 420 nm) resulted from the luminol excitation by $HO^{\bullet}$ radicals (which came up from H_2O_2 decomposition) was measured with a *Turner BioSystems Modulus* single tube luminometer.

Table 1
Structural and textural properties of the catalysts.

Catalyst	Metal content (wt%)	Surface area S_{BET} (m^2 g^{-1})	Phase composition	Point of zero charge
CuO/Al_2O_3	9.55	215	CuO, $\eta(\gamma)$ Al_2O_3	7.75
NiO/Al_2O_3	9.70	203	NiO, $\eta(\gamma)$ Al_2O_3	7.43
Al_2O_3	–	247	$\eta(\gamma)$ Al_2O_3	7.29

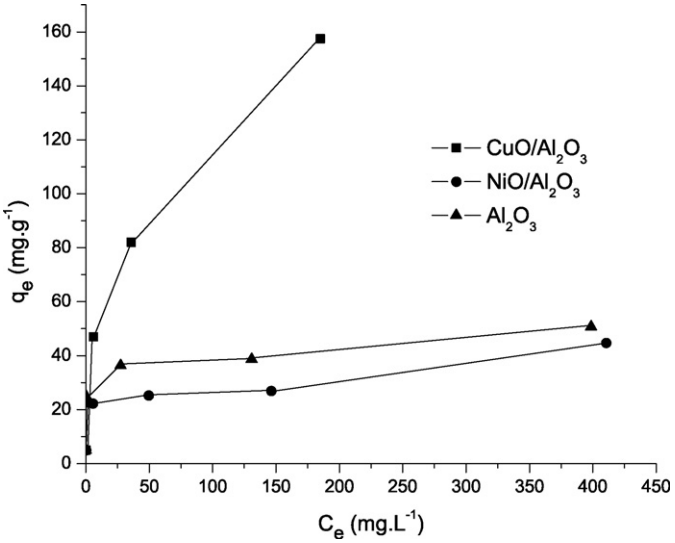

Fig. 2. Adsorption isotherms of RB5 onto CuO/Al_2O_3, NiO/Al_2O_3 and Al_2O_3 (pH 5.5, temperature = 21 °C).

3. Results and discussion

3.1. Adsorption of RB5 onto the catalysts

Adsorption capacity of the CuO/Al_2O_3, NiO/Al_2O_3 and of alumina support toward RB5 is illustrated by the adsorption isotherm at pH 5.5 (Fig. 2). It is worthy to note that the alumina and the NiO/Al_2O_3 catalyst present a moderate adsorption capacity in comparison with CuO/Al_2O_3. The adsorption isotherm for copper based catalyst has a high slope, indicating a considerable adsorption capability even at low equilibrium dye concentration.

The experimental equilibrium data are fitted to the Langmuir isotherm:

$$\frac{1}{q_e} = \frac{1}{Q_m b}\frac{1}{C_e} + \frac{1}{Q_m} \quad (1)$$

where C_e is the equilibrium concentration, q_e the amount of material adsorbed at equilibrium, b the affinity parameter or Langmuir constant and Q_m the capacity parameter.

Freundlich isotherm was also used to fit the data:

$$\log\ q_e = \log K_F + \frac{1}{n}\log C_e \quad (2)$$

In Eq. (2), K_F is the Freundlich adsorption constant and $1/n$ depends on the linearity of the isotherm and varies between 0 and 1.

Adsorption coefficients of both model isotherms are presented in Table 2. The results show that Langmuir model adequately describes the adsorption equilibrium of RB5 onto alumina and NiO/Al_2O_3. Instead, the adsorption isotherm of RB5 onto CuO/Al_2O_3 is very well fitted to Freundlich model indicating a heterogeneous surface indeed for this catalyst. In fact, a good fit should indicate the existence of at least two types of surface centers, ones belonging to the support and the others, to the copper oxide (see further discussions).

The values of adsorption constant show a relatively easy uptake of dye molecules on catalysts surface. Also these data reveal that copper oxide deposition onto alumina surface induces a significant increase of adsorption properties comparing with nickel based catalyst, which has even lower affinity than alumina. This behavior might suggests that copper oxide deposition causes the appearance of new adsorption centers with high complexing capacity while nickel oxide covers some adsorption sites on alumina surface, which result in a decrease of the overall sorption properties.

The point of zero charge (PZC) for all the three solids is superior to 7.2. This means that at the operational pH (5.5) the surface is positively charged. For the alumina, surface acid–base equilibrium can be described as follows:

$$Al\text{–}OH_2^+ \underset{+H^+}{\overset{-H^+}{\rightleftarrows}} Al\text{–}OH \underset{+H^+}{\overset{-H^+}{\rightleftarrows}} Al\text{–}O^-$$

Taking into account the pK_a value of 10.16 for RB5, at pH 5.5 the interaction would occur between $Al\text{–}OH_2^+$ and the dye in the molecular form (pK_a > pH). The partial negative charges for RB5 molecule calculated by Garcia et al. [36] indicate that the adsorption of the azoic dye on a positively charged surface occurs via the groups with larger density of electronic charges: sulfonate (−0.8677), sulfate (−0.8641), sulfonilic (−0.8294) and hydroxyl (−0.2496). Sulfonate group is considered the principal responsible for the RB5 adsorption onto a positively charged surface also by Karadag et al. [37].

We have used infrared spectroscopy to put in evidence the surface species on our catalysts. Thus, DRIFT spectra were obtained for the RB5 adsorbed onto NiO/Al_2O_3 and CuO/Al_2O_3 and illustrated in Fig. 3: parts (a) and (c). Similar peaks are revealed, but the intensity of part of these peaks for CuO/Al_2O_3 catalyst is higher. In order to assign these peaks to different vibration modes, we considered the characteristic absorptions given by the different vibrating groups of our systems. Table 3 collects the expected absorptions as indicated in the more or less classic literature e.g. [38–43].

Therefore, most of the IR peaks observed in our spectra were assigned as follows: the peaks 1595–1593, 1576–1574 and 1499–1497 cm^{-1} correspond to the aromatic ring stretching vibrations, that at 1251–1218 cm^{-1} to stretching vibration of phenolic C–O bond, at 1344–1341 cm^{-1}, to the stretching of sulfate and sulfonate groups. The $-SO_2-$ symmetric stretching vibration appears at 1182–1140 cm^{-1} for both sulfonate and sulfate groups.

These observations sustain the adsorption of RB5 on our CuO and NiO supported catalysts, preponderantly via sulfonate ($-SO_3^-$) and sulfate ($-SO_4^-$) groups. The higher adsorption capacity of CuO/Al_2O_3 than of NiO/Al_2O_3 is most probably due to the formation of a copper–RB5 complex. In fact, the capacity of azo dyes to form complexes with copper is well known. Some of them are produced as pre-metallized copper complex dyes (i.e. formazan copper complexes) [44]. To investigate the formation of the metal-dye complex in our case, $Cu(NO_3)_2$ or $Ni(NO_3)_2$ were dissolved in a RB5 solution of 10 mg L^{-1} in an amount ensuring the molar ratio of 100:1. As can be seen from the corresponding UV–vis absorption spectra (Fig. 4), RB5 presents main absorption bands at 312, 392 and 599 nm while

Table 2
Parameters of RB5 adsorption isotherms onto catalysts and alumina support.

Solid sample	Langmuir model			Freundlich model		
	Q_m (mg g^{-1})	b (L mg^{-1})	r^a	K_F (mg$^{1-1/n}$/L$^{-1/n}$ g^{-1})	$1/n$	r^a
CuO/Al_2O_3	91.2	0.36	0.9696	23.8	0.35	0.9988
NiO/Al_2O_3	29.3	0.90	0.9958	9.07	0.26	0.9452
Al_2O_3	71.12	1.55	0.9825	24.2	0.11	0.9766

[a] r is the linear correlation coefficient.

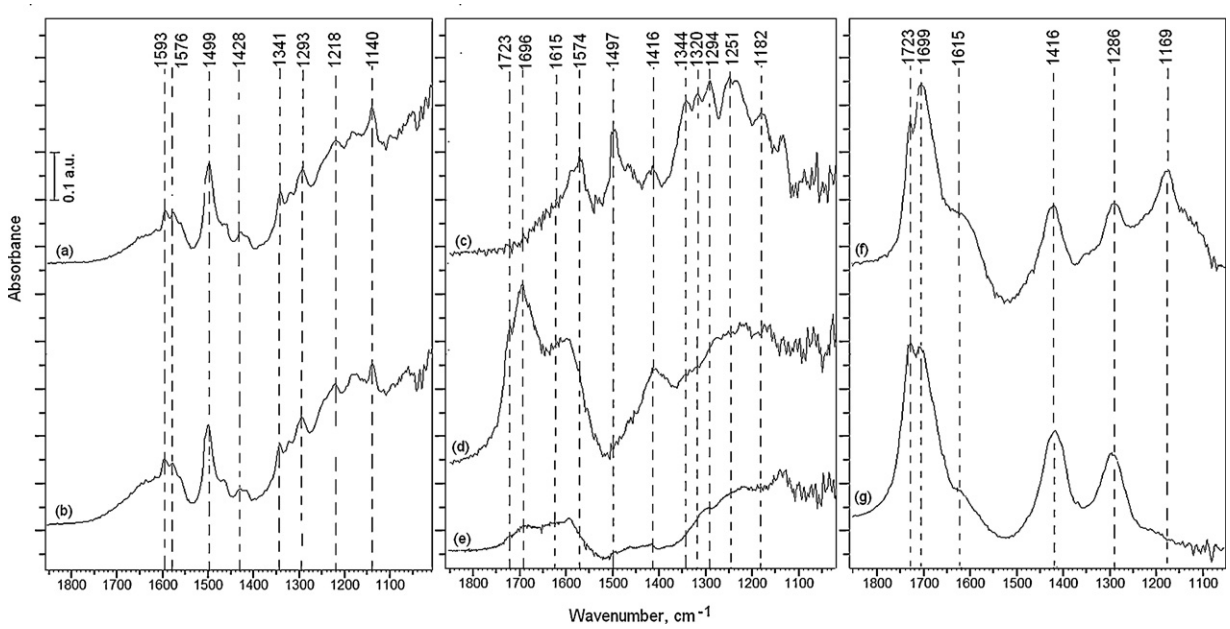

Fig. 3. DRIFT spectra in the region 1000–1900 cm^{-1} for NiO/Al_2O_3: (a) RB5 adsorption, (b) RB5 oxidation (after 4 h), and for CuO/Al_2O_3: (c) RB5 adsorption, (d) RB5 oxidation (after 2 h), (e) RB5 oxidation (after 4 h), (f) RB5 oxidation (after 1 h), (g) oxalic acid adsorption.

Table 3
Expected characteristic peaks in the infrared spectrum of RB5.

Absorption peaks cm^{-1}	Assignment	Observations[a]
3600–3640	O–H stretching in free OH groups	s
3200–3500	O–H stretching in H bonded OH groups	s, b
3400–3250	Stretching of N–H bond in NH_2 groups	m
3100–3000	C–H stretching in benzene ring	m
2925	C–H asymmetric stretching in CH_2 groups	m
2860	C–H symmetric stretching in CH_2 groups	m
2000–1700	Overtones and combination vibrations of benzene ring	w
1650–1560	NH_2 bending	m
1603, 1583	8a, 8b CC stretching in benzene ring	m
1498, 1460	19a, 19b CC stretching in benzene ring	m
1470–1450	Deformation of the CH_2 groups	m
1400–1530	N=N stretching of asymmetric azo group	vw
1370–1350	CH_2 rocking	m
1335–1250	C–N stretching in aromatic amines	s
1350–1330	Sulfone SO_2 stretching	s
1320–1000	C–O stretching	s
1174 (1226, 1122)	ν_3 stretching of the SO4 group	vs (sh)
1160–1120	Sulfone SO_2 stretching	s
1130–1070	Sulfoxide SO stretching	s
885, 850	Vibrational modes of $[HSO_4]^-$ anion	
843	10a mode out-of-plane of benzene ring	
613, 659	ν_4 stretching of the SO_4 group	
454, 409	ν_2 stretching of the SO_4 group	

[a] m = medium; s = strong; sh = shoulder; v = very; w = weak.

the copper ion containing RB5 solution shows absorptions at 278, 359 and 527 nm, the wavelength shift indicating the involvement of lone pair electrons in coordination bonds. Moreover, coordination affects the whole π electron system of the dye molecule and the corresponding absorption bands are shifted. Instead, nickel containing solution shows only very small changes especially in the shortest UV region determined by π–π* transitions in the aromatic part of the dye molecule; no clear coordination can be inferred.

3.2. Catalytic oxidation of RB5

3.2.1. Oxidation tests

Firstly, the oxidation tests of the aqueous solution of RB5 (100 mg L^{-1}) were carried out using H_2O_2 at a concentration of 40 mM. It was found that in the absence of a catalyst, the RB5 removal did not take place. Instead, for the catalytic process the RB5 concentration decreases in time for both catalytic systems. The

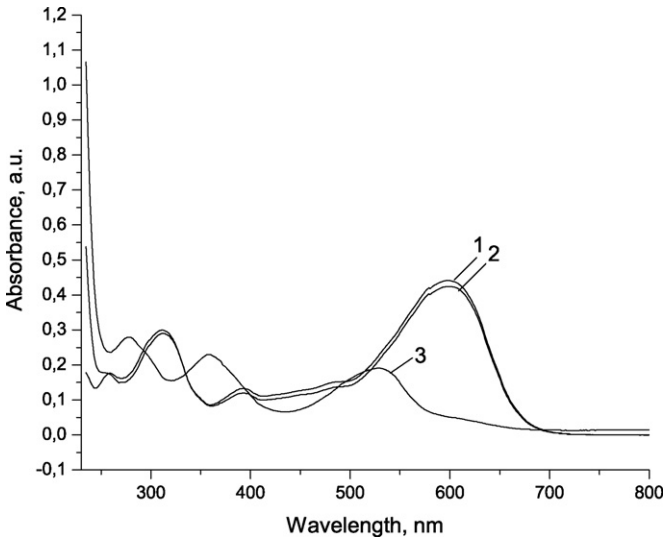

Fig. 4. The UV–vis absorption spectra of: (1) RB5; (2) RB5 and $Ni(NO_3)_2$ in the molar ratio of 1:100; (3) RB5 and $Cu(NO_3)_2$ in the molar ratio of 1:100.

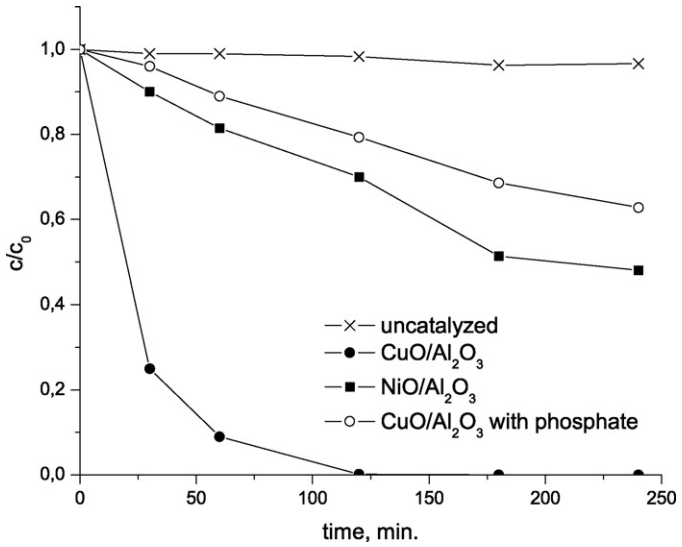

Fig. 5. Oxidation of RB5 in the presence or absence of catalysts (H_2O_2 concentration = 40 mM; initial concentration of RB5, C_0 = 100 mg L^{-1}; pH 5.5).

decrease is more important for the CuO/Al_2O_3 (above 90% in 1 h) in comparison with NiO/Al_2O_3 (about 20%) (Fig. 5).

These results are in accordance with other literature data. Thus, Qiu et al. [24] found similar differences between the catalytic activity of impregnated CuO and NiO supported on γ-Al_2O_3 in the oxidation of another azo dye, Acid Scarlet GR, with hydrogen peroxide (without considering the possible dye adsorption on the catalysts).

To evaluate the RB5 degradation degree we performed TOC measurements. The TOC values decrease, but the RB5 concentration/TOC ratio remains almost constant during the process onto NiO/Al_2O_3, while onto CuO/Al_2O_3 this ratio clearly diminishes (Fig. 6). These results suggest that for CuO/Al_2O_3 the dye removal occurs with formation of small molecular weight compounds, while for NiO/Al_2O_3 the RB5 removal is mainly due to the adsorption onto the catalyst. This explanation is supported by the IR analysis of the surface species onto the catalysts after adsorption and after oxidation of RB5.

Thus, the DRIFT spectrum of NiO/Al_2O_3 on which RB5 was adsorbed is almost identical with spectrum of NiO/Al_2O_3, which was used for 4 h in oxidation process (Fig. 3(a) and (b)). Instead,

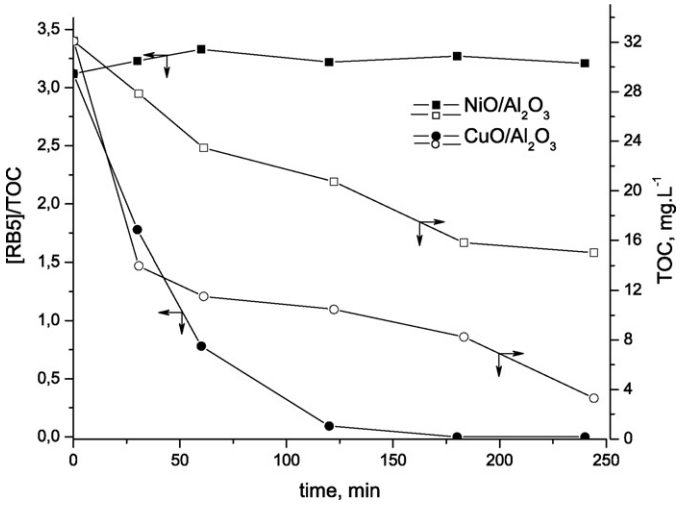

Fig. 6. Evolution in time of TOC and [RB5]/TOC ratio (H_2O_2 concentration = 40 mM, pH 5.5).

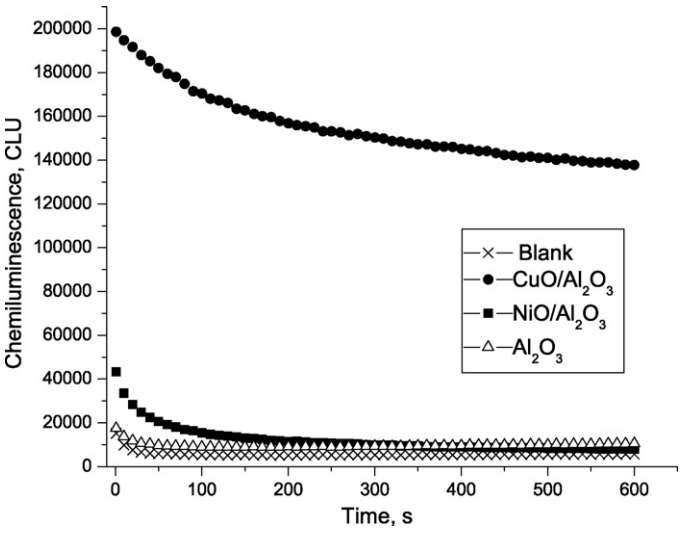

Fig. 7. Chemiluminescence measurements for CuO/Al_2O_3, NiO/Al_2O_3 and Al_2O_3.

after 1–2 h reaction, the DRIFT spectra of CuO/Al_2O_3 catalyst reveal not only adsorbed RB5 but also other surface species containing especially COO^- group (Fig. 3(d) and (f)). The strong peaks, which appear in the region 1723–1615 cm^{-1}, correspond to asymmetric stretching vibration of carboxylic group and that at 1286 cm^{-1} to –C–O stretching vibration. The peak at 1416 cm^{-1}, which strongly increases, might be also due to the stretching of carboxylate (symmetric one) but of NH^+ ammonium stretching [45] as well. The current pH seems to favor the latter assignment; however, more investigations are necessary to unravel this assignment.

The band at 1169 cm^{-1} indicates that after 1-h reaction there are still surface species containing sulfate and/or sulfonate groups. Due to the disappearance of the peaks in the region 1500–1450 cm^{-1}, the breakage of the azo bond and the destruction of the aromatic rings might be assumed as main steps in the catalytic oxidation pathway of RB5.

This evolution confirms the degradation of RB5 onto CuO/Al_2O_3 with formation of oxidation by-products, preponderantly carboxylic acids. In addition, the spectra of CuO/Al_2O_3 after 1 h reaction (Fig. 3(f)) was compared to the spectra of oxalic acid adsorbed onto CuO/Al_2O_3 (Fig. 3(g)). A good match was observed for the two spectra in the region 1800–1200 cm^{-1}, sustaining the formation of carboxylic acid on the catalyst surface during the RB5 oxidation.

After 4 h of reaction, the characteristic peaks of adsorbed RB5 and possibly of by-products cannot be observed (Fig. 3(e)) suggesting either their removal from the CuO/Al_2O_3 surface or an overloading of several surface species, which disturbs discerning the peaks.

3.2.2. Radical generation during the reaction

Chemiluminescence measurements were carried out to evaluate the capacity of catalysts to generate hydroxyl radicals since the chemiluminescence signal is proportional with the yield of $HO^\bullet$ in the system [35]. A pro-oxidative character was observed only for CuO/Al_2O_3 catalyst, as the intensity of chemiluminescence signal was one order of magnitude higher than that obtained for NiO/Al_2O_3 (Fig. 7). Peroxide hydrogen decomposition with generation of hydroxyl radicals, in the presence of copper oxide catalysts has been also revealed through chemiluminescence measurements by Drijvers et al. [46]. The higher capacity of CuO/Al_2O_3 to generate $HO^\bullet$ radicals, comparing to NiO/Al_2O_3 can be caused by the difference between the reduction potentials of the systems Cu^{2+}/Cu^+ and Ni^{2+}/Ni^0 (E Cu^{2+}/Cu^+ = 0,167 eV; E Ni^{2+}/Ni^0 = −0.25 eV) as Roy

stressed [47]. This behavior can explain the lack of activity for the NiO/Al_2O_3 in the RB5 oxidation with hydrogen peroxide.

3.2.3. Effect of H_2O_2 dose

The effect of the oxidizing agent dose on the catalytic oxidation process was investigated for the H_2O_2 concentrations from 10 to 60 mM.

In the presence of NiO/Al_2O_3, the amount of RB5 removed from the aqueous solution is the same irrespective of H_2O_2 concentration, also sustaining that the dye is eliminated from the solution only by adsorption.

The data illustrated in Fig. 8 show a low influence of the H_2O_2 concentration on the process catalyzed by CuO/Al_2O_3. Nevertheless, a significant variation of the RB5 with the hydrogen peroxide dose can be observed for the first 30 min. The amount of the RB5 degraded increases with the peroxide hydrogen dose until a concentration of 40 mM is reached. Further rise of H_2O_2 concentration did not yield a greater conversion of the azoic dye.

At rather high concentrations, hydrogen peroxide can act as a scavenger of hydroxyl radicals [30,48,49]:

$$H_2O_2 + HO^\bullet \rightarrow HO_2^\bullet + H_2O$$

$$HO_2^\bullet + HO^\bullet \rightarrow H_2O + O_2$$

diminishing the efficiency of the organic substrate degradation. This fact might explain why runs carried out at different initial concentration of hydrogen peroxide are rather similar.

We have already seen that the adsorption data (Figs. 2 and 4) denote that the adsorption of the dye molecules occurs on the alumina and especially on the CuO sites. The chemiluminescence measurements put in evidence that in the hydrogen peroxide decomposition, CuO is the active phase. Therefore, a competition between the RB5 and H_2O_2 for the active sites would be expected. This competition is further sustained by the highest rate of the H_2O_2 decomposition reached in the absence of the dye in comparison with the rate of H_2O_2 consumption in the RB5 oxidation process

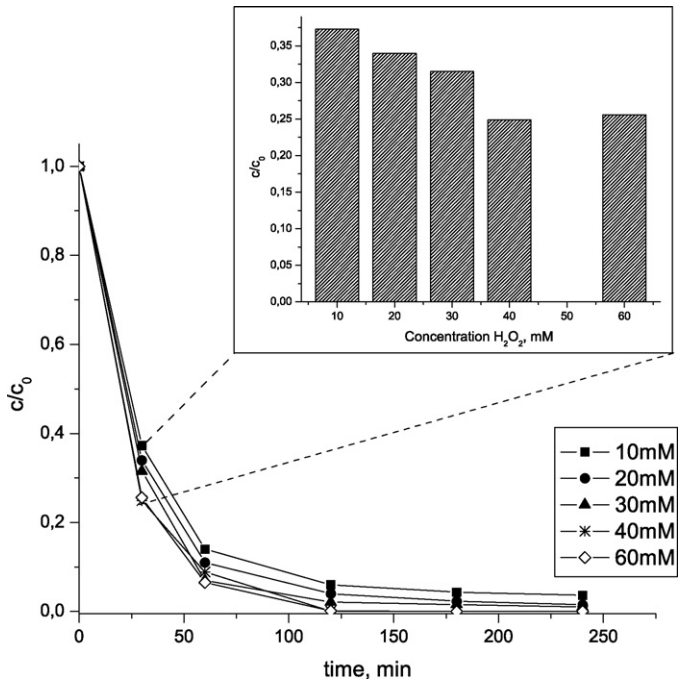

Fig. 8. Influence of H_2O_2 concentration on RB5 oxidation in presence of CuO/Al_2O_3 (initial concentration of RB5, $C_0 = 100\ mg\ L^{-1}$).

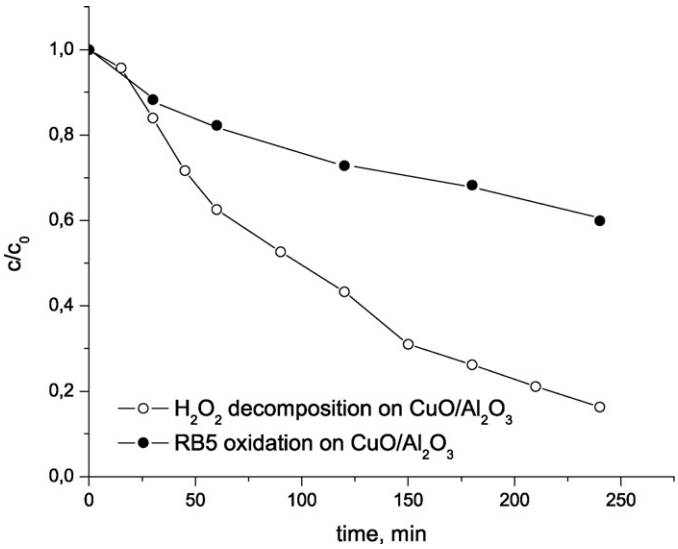

Fig. 9. Evolution of the H_2O_2 concentration in the H_2O_2 decomposition and RB5 oxidation catalytic processes (initial concentration H_2O_2, $C_0 = 40$ mM; pH 5.5).

(Fig. 9) and may be an additional reason for the small increment of the RB5 degradation with the H_2O_2 dose.

3.2.4. Effect of phosphate ions

The industrial wastewaters with organic load contain often some inorganic compounds that can affect the oxidative treatment processes. In the case of wastewater from textile industry beside dyes, detergent constituents like phosphates may be present.

In order to determine if the phosphate ions influence the oxidative degradation RB5, a mixture of NaH_2PO_4: Na_2HPO_4: H_3PO_4 in the molar ratio of 90:7:3 was added to the aqueous solution of dye. The total concentration of phosphate ions was 40 mM; the pH was 5.5 as in the initial oxidation tests.

In the presence of phosphate ions the dye conversion drops with 60–80% indicating a strong inhibiting effect of these species on the catalytic oxidation of RB5 (Fig. 5).

We have to notice that, in water pollutants oxidation processes with ozone or hydrogen peroxide, phosphate buffers are sometimes used in order to keep a constant pH [50–52]. Moreover, the phosphate ions are considered as promoters in ozonation processes occurring by hydroxyl radicals as well [53]. However, Pi et al. [54] revealed an obvious inhibiting effect of phosphate buffer on the catalyzed ozonation of oxalic acid. For the oxidation of Durazol Blue 8 G with hydrogen peroxide in alkaline medium (pH > 9), El-Daly et al. [55] found that the rate constant is greater when the pH correction was achieved with NaOH or a buffer tetraborate/NaOH than that with phosphate buffer. In addition, Kim et al. [56] found that phosphate ions are good H_2O_2 stabilizers. A poisoning effect of phosphates on the catalyst cannot be excluded and this hypothesis was also advanced by Pi et al. [54].

Our results are in accordance with the above-mentioned literature data. Moreover, the DRIFT spectrum of CuO/Al_2O_3 which was in contact with a RB5 solution buffered with phosphate presents peaks at 1182 cm^{-1} and at 975 cm^{-1} characteristic for P=O and P–O stretching vibration respectively, revealing the phosphate adsorption on the catalyst (Fig. 10).

3.2.5. Kinetics of the RB5 oxidation on CuO/Al_2O_3

As it was previously shown, only CuO/Al_2O_3 was active in the degradation of the RB5. So, the kinetics evaluation of the oxidation process is made only for this catalyst.

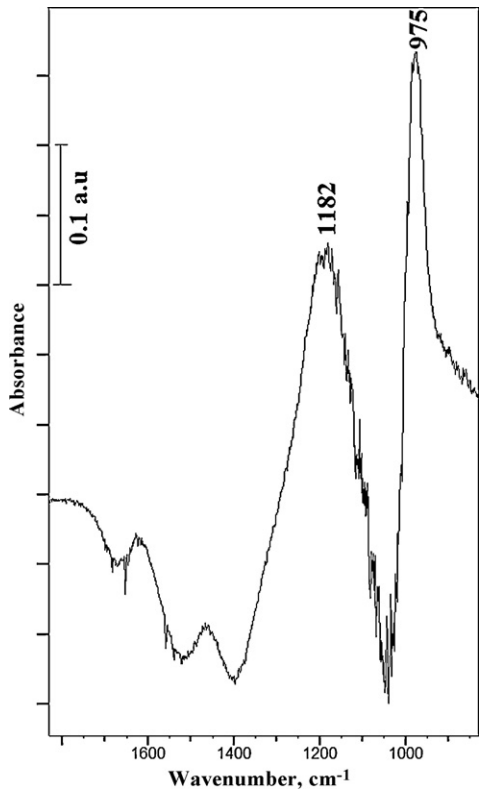

Fig. 10. DRIFT spectrum of phosphate adsorbed on CuO/Al_2O_3.

Since the oxidation of the dye was not observed in the absence of the catalyst, a direct reaction between hydrogen peroxide and dye molecules was no more considered. Consequently, assuming that the hydroxyl radical is the main oxidation species, the overall rate of the RB5 degradation can be expressed as:

$$\frac{-\mathrm{d}[\mathrm{RB5}]}{\mathrm{d}t} = k''[\mathrm{RB5}][\mathrm{HO}^\bullet] \quad (3)$$

where k″ is a second order rate constant.

As commonly is assumed, in the presence of excess of hydrogen peroxide (fivefold in our case), the concentration of the hydroxyl radicals can be considered constant [57]. Thus, the rate equation can be simplified into a pseudo-first order as follows:

$$\frac{-\mathrm{d}[\mathrm{RB5}]}{\mathrm{d}t} = k_{\mathrm{obs}}[\mathrm{RB5}] \quad (4)$$

where k_{obs} is a first order rate constant.

We found that the pseudo-first order kinetic model fit indeed our experimental data. The k_{obs} obtained from the slope of the plot of $\ln([RB5]/[RB5]_0)$ versus time is 0.039 min^{-1} (Fig. 11). One can see that our k_{obs} has rather high value, comparable with other literature values found in conditions more or less similar with ours (Table 4).

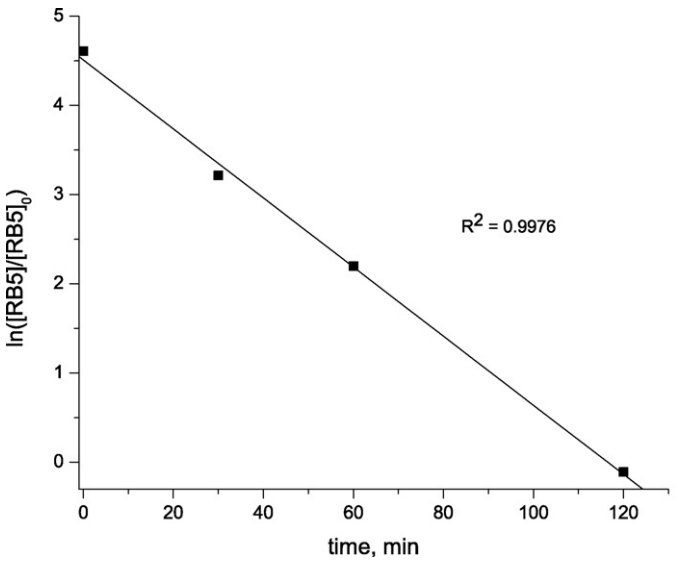

Fig. 11. A first order rate representation for the RB5 oxidation on CuO/Al_2O_3 (H_2O_2 concentration = 40 mM; initial concentration of RB5, C_0 = 100 mg L^{-1}; pH 5.5).

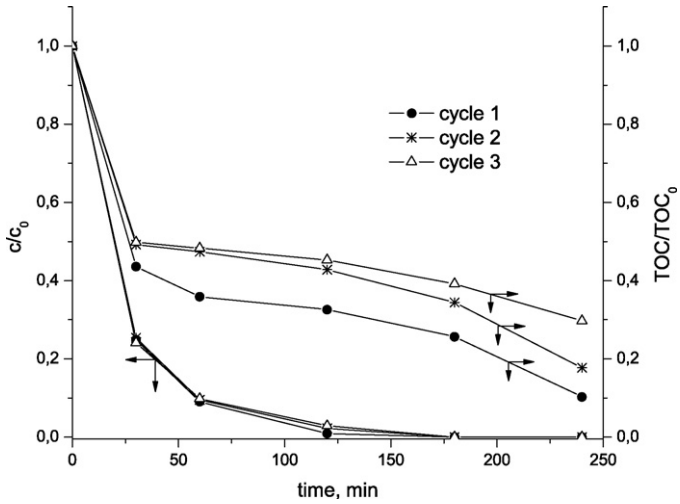

Fig. 12. Oxidation of RB5 on CuO/Al_2O_3 in three consecutive reaction cycles (H_2O_2 concentration = 40 mM; initial concentration of RB5, C_0 = 100 mg L^{-1}; TOC_0 = 32.1 mg L^{-1}; pH 5.5).

3.2.6. Catalyst stability

In order to test the stability of the CuO/Al_2O_3 in the RB5 oxidation process, repetitive reaction (up to three runs) was performed. For that, the catalyst was recovered by filtration after each run, then dried and weighted in order to use the appropriate amount in the next cycle. The catalyst stability was also evaluated by determining the amount of copper leached from catalyst during the dye oxidation.

Table 4
Pseudo-first order rate constant for oxidation of RB5 and other azo dyes.

AOP type	Experimental parameters	k_{obs} (min^{-1})	Ref.
Electro-Fenton	$[RB5]_0$ = 100 mg L^{-1} (0.1 mM); potential = −0.55 V/SCE; pH 3; t = not specified	0.019	[58]
H_2O_2/(iron oxide/sand)	$[RB5]_0$ = 500 mg L^{-1} (0.5 mM); $[H_2O_2]_0$ = 16 mM; pH 4; t = 20 °C and 30 °C	0.0033–0.0377 (depending on the temperature)	[27]
H_2O_2/mixed oxides of iron and silica	$[Methyl\ red]_0$ = 0.05 mM; H_2O_2/Fe (molar ratio) = 20; pH 5 and 7; t = 20 °C	0.002–0.110 (depending on the catalyst and on the pH)	[26]
H_2O_2/(Fe/aerogel C)	$[Orange\ II]_0$ = 0.1 mM; $[H_2O_2]_0$ = 6 mM; pH 3; t = 30 °C	0.189–0.079 (depending on the cycle)	[31]
H_2O_2/(metal complex)	$[Acid\ orange\ 7]_0$ = 0.1 mM; $[H_2O_2]_0$ = 30 mM; pH 8; t = 25 °C	0.0013–0.0220 (depending on the catalyst)	[59]

Table 5
Copper leaching from CuO/Al_2O_3 during RB5 oxidation (initial of RB5 concentration = 100 mg L^{-1}; H_2O_2 concentration = 40 mM; pH 5.5).

Cycle	Time (min)	Copper leached (mg L^{-1})	Amount of copper lost (%)
	30	2.01	
	60	2.00	
1st	120	2.53	
	180	2.81	
	240	3.09 (total loss in 1st cycle)	1.62
2nd	240	2.31	1.21
3rd	240	1.85	0.97

As can be seen from Fig. 12, the catalyst performance is less affected in terms of RB5 concentration between the three cycles. Moreover, the corresponding kinetic constants only slightly diminish from 0.039 to 0.031 min^{-1} and then to 0.029 min^{-1} in the third run. Nevertheless, the degree of the dye mineralization (evaluated in terms of TOC reduction) decreases with the number of cycles from 90.1% to 70.3% for the last cycle (Fig. 12).

One of the reasons for the activity decay may be the copper leaching, however this achieved only 1.0–1.6% per cycle from the initial amount present in the catalyst (Table 5). Since the decrease of the mineralization degree of the dye is important and cannot be caused only by this moderate leaching of the active component, then it can have another reason, for example by the covering of active sites of CuO/Al_2O_3 by adsorption of some partial degradation products. Therefore, a catalyst reactivation is necessary after a number of cycles. Studies devoted to the regeneration and improvement of the catalyst stability are thus necessary.

4. Conclusions

RB5 oxidation with hydrogen peroxide was performed in aqueous solution over CuO/Al_2O_3 and NiO/Al_2O_3 catalysts. The evolution of RB5 concentration/TOC ratio and especially the comparative analysis of DRIFT spectra reveal a different behavior of the two catalytic systems. Thus, RB5 can be effectively degraded by oxidative way in the presence of CuO/Al_2O_3. On the contrary, RB5 removal is the result of a simple adsorption phenomenon for the process carried out in the presence of NiO/Al_2O_3. The different behavior of the two catalytic systems might be explained through the lack of activity of NiO/Al_2O_3 in the generation of $HO^{\bullet}$ radicals. Furthermore, the adsorption data show differences between CuO/Al_2O_3 and NiO/Al_2O_3. The important adsorption capacity of CuO/Al_2O_3 was explained by the formation of a cooper-RB5 complex.

In the process carried out in the presence of CuO/Al_2O_3 with a H_2O_2 concentration of 40 mM the azo dye was completely eliminated from both solution and catalyst surface after 4 h, with a TOC abatement greater than 90%. The variation from 10 to 60 mM of the H_2O_2 concentration has a slight influence on the catalytic process. For the first 30 min of reaction an optimal concentration for the oxidizing agent of 40 mM can be considered.

The analysis of the DRIFT spectra of the copper based catalyst surface at different time reveals that at least a part of oxidation by-products were also adsorbed. Carboxylic acids are probably the mostly adsorbed by-products. However, carboxylic acids are not the only intermediate surface species identified; species containing sulfate and/or sulfonate are also present.

In the conditions of hydrogen peroxide excess, the rate equation in the case of copper catalyst was simply expressed by a pseudo-first order equation and the model was found to fit the data. The rate constant estimated has a reasonable and rather high value.

The oxidation process is influenced by the presence of some inorganic anions. Thus, it was found that phosphate ions effectively inhibit the oxidative degradation of RB5 due to their strong adsorption on the catalysts.

The catalyst stability was evaluated by determining the amount of copper leached from catalyst during the dye oxidation. It was established that the copper leaching reached only 1.0–1.6% per cycle from the initial amount present in the catalyst. The high decrease of the mineralization degree with the number of cycles speaks instead about adsorption of some by-products onto the catalyst surface, covering the active centers.

Acknowledgement

Financial support from the Romanian Ministry of Education and Research under PN II 22110 Project is gratefully acknowledged.

References

[1] A. Telke, D. Kalyani, J. Jadhav, S. Govindwar, Acta Chim. Slov. 55 (2008) 320–329.
[2] H.M. Pinheiro, E. Touraud, O. Thomas, Dyes Pigments 61 (2004) 121–139.
[3] M.H. Enzari, Z. Sharif al-Hoseini, N. Ashraf, Ultrason. Sonochem. 15 (2008) 433–437.
[4] H.S. Weinberg, W.H. Glaze, Water Res. 31 (1997) 1555–1572.
[5] M.S. Lucas, A.A. Dias, A. Sampaio, C. Amaral, J.A. Peres, Water Res. 41 (2007) 1103–1109.
[6] R. Munter, Proc. Est. Acad. Sci. Chem. 50 (2001) 59–80.
[7] R. Andreozzi, V. Caprio, R. Marotta, V. Tufano, Water Res. 35 (2001) 109–120.
[8] M. Pera-Titus, V. García-Molina, M. Baños, J. Giménez, S. Esplugas, Appl. Catal. B 47 (2004) 219–256.
[9] N. Azbar, T. Yonar, K. Kestioglu, Chemosphere 55 (2004) 35–43.
[10] A. Burbano, D. Dionysiou, M. Suidan, T. Richardson, Water Res. 39 (2005) 107–118.
[11] B. Légube, N. Karpel Vel Leitner, Catal. Today 53 (1999) 61–72.
[12] I. Udrea, C. Bradu, Ozone: Sci. Eng. 25 (2003) 335–343.
[13] F. Beltrán, F. Rivas, R. Montero-de-Espinosa, Appl. Catal. B 47 (2004) 101–109.
[14] M. Taralunga, J. Mijoin, P. Magnoux, Appl. Catal. B 60 (2005) 163–171.
[15] Q. Yang, H. Choi, Y. Chen, D. Dionysiou, Appl. Catal. B 77 (2008) 300–307.
[16] J.A. Melero, F. Martínez, J.A. Botas, R. Molina, M.I. Pariente, Water Res. 43 (2009) 4010–4018.
[17] J. Barrault, M. Abdellaoui, C. Bouchoule, A. Majesté, J.M. Tatibouët, A. Louloudi, N. Papayannakos, N.H. Gangas, Appl. Catal. B 27 (2000) L225–L230.
[18] M. Constapel, M. Schellenträger, J.M. Marzinkowski, S. Gäb, Water Res. 43 (2009) 733–743.
[19] Y. Flores, R. Flores, A.A. Gallegos, J. Mol. Catal. A 281 (2008) 184–191.
[20] S. Meriç, D. Kaptan, T. Ölmez, Chemosphere 54 (2004) 435–441.
[21] J.H. Sun, S.P. Sun, G.L. Wang, L.P. Qiao, Dyes Pigments 74 (2007) 647–652.
[22] M. Surpăţeanu, C. Zaharia, Cent. Eur. J. Chem. 2 (2004) 573–588.
[23] X.R. Xu, H.B. Li, W.H. Wang, J.D. Gu, Chemosphere 57 (2004) 595–600.
[24] Z. Qiu, Y. He, X. Liu, S. Yu, Chem. Eng. Process. 44 (2005) 1013–1017.
[25] Y. Liu, D. Sun, J. Hazard. Mater. 143 (2007) 448–454.
[26] K. Hanna, T. Kone, G. Medjahdi, Catal. Commun. 9 (2008) 955–959.
[27] C.P. Huang, Y.F. Huang, H.P. Cheng, Y.H. Huang, Catal. Commun. 10 (2009) 561–566.
[28] M. Neamţu, C. Catrinescu, A. Kettrup, Appl. Catal. B 51 (2004) 149–157.
[29] N.N. Fathima, R. Aravindhan, J.R. Rao, B.U. Nair, Chemosphere 70 (2008) 1146–1151.
[30] J.H. Ramirez, F.J. Maldonado-Hódar, A.F. Pérez-Cadenas, C. Moreno-Castilla, C.A. Costa, L.M. Madeira, Appl. Catal. B 75 (2007) 312–323.
[31] F. Duarte, F.J. Maldonado-Hódar, A.F. Pérez-Cadenas, L.M. Madeira, Appl. Catal. B 85 (2009) 139–147.
[32] R. Šuláková, R. Hrdina, G.M.B. Soares, Dyes Pigments 73 (2007) 19–24.
[33] S.M. Avramescu, N. Mihalache, C. Bradu, M. Neata, I. Udrea, Catal. Lett. 129 (2009) 273–280.
[34] G.M. Eisenberg, Ind. Eng. Chem. Anal. Ed. 15 (1943) 327–328.
[35] M. Voicescu, G. Ioniţă, T. Constantinescu, M. Vasilescu, Rev. Roum. Chim. 51 (2006) 683–690.
[36] J. Garcia, M. Boroski, A. da Silva, J. Oliveira, J. Nozaki, W. Barreto, in: T.P. Hough (Ed.), Solar and Trends in Solar Energy Research, Nova Science Publishers Inc., New York, 2006, pp. 107–132.
[37] D. Karadag, M. Turan, E. Akgul, S. Tok, A. Faki, J. Chem. Eng. Data 52 (2007) 1615–1620.
[38] M. Avram, G.H. Mateescu, Infrared Spectroscopy: Applications in Organic Chemistry, Wiley-Interscience, New York, 1966.
[39] B. Schrader, Raman/Infrared Atlas of Organic Compounds, 2nd edition, VCH, Weinheim, 1989.
[40] P.M. Fedorak, D. Grbic-Galic, Appl. Environ. Microbiol. 57 (1991) 932–940.
[41] W.O. George, R.C.W. Goodman, J.H.S. Green, Spectrochim. Acta 22 (1966) 1741–1749.
[42] G.W. Rayner-Canham, D. Sutton, Can. J. Chem. 49 (1971) 3994–3996.
[43] M. Belhouchet, M. Bahri, J.M. Savariault, T. Mhiri, Spectrochim. Acta Part A 61 (2005) 387–393.

[44] H. Zollinger, Color Chemistry. Syntheses, Properties, and Applications of Organic Dyes and Pigments, 3rd edition, Wiley–VCH, Zürich, 2003.
[45] P. Fusi, G.G. Ristori, A. Malquori, Clay Miner. 15 (1980) 147–155.
[46] D. Drijvers, H. Van Langenhove, M. Beckers, Water Res. 33 (1999) 1187–1194.
[47] C.B. Roy, J. Catal. 12 (1968) 129–133.
[48] L. Carlos, D. Fabbri, A.L. Capparelli, A.B. Prevot, E. Pramauro, F.G. Einschlag, J. Photochem. Photobiol. A 201 (2009) 32–38.
[49] M. Neamtu, I. Siminiceanu, A. Yediler, A. Kettrup, Dyes Pigments 53 (2002) 93–99.
[50] R. Andreozzi, A. Insola, V. Caprio, M.G. D'Amore, Water Res. 26 (1998) 917–921.
[51] J. Ma, N.J.D. Graham, Water Res. 34 (2000) 3822–3828.
[52] F. Erol, T. Özbelge, Chem. Eng. J. 139 (2007) 272–283.
[53] F.J. Rivas, F. Beltrán, O. Gimeno, F. Carvalho, J. Environ Sci. Health Part A: Toxic/Hazard. Subst. Environ. Eng. 38 (2003) 371–379.
[54] Y. Pi, M. Ernst, J.C. Schrotter, Ozone: Sci. Eng. 25 (2003) 393–397.
[55] H. El-Daly, A.F. Habib, M. Borhan El-Din, Dyes Pigments 57 (2003) 197–210.
[56] S.Y. Kim, N.H. Kim, J.H. Lim, E.G. Chang, Electron. Lett. 39 (2003) 718–719.
[57] H.Y. Shu, M.C. Chang, H.J. Fan, J. Hazard. Mater. B 113 (2004) 201–208.
[58] E. Kusvuran, S. Irmak, H.I. Yavuz, A. Samil, O. Erbatur, J. Hazard. Mater. B 119 (2005) 109–116.
[59] J. Tokuda, R. Oura, T. Iwasaki, Y. Takeuchi, A. Kashiwada, M. Nango, JSDC 116 (2000) 42–47.